DOI: 10.1002/ejic.200700091

Pyridine Carboxylate Complexes of Mo^{II} as Active Catalysts in Homogeneous and Heterogeneous Polymerization

Maria Vasconcellos-Dias,[a] Carla D. Nunes,*[a] Pedro D. Vaz,[a] Paula Ferreira,[b] and Maria José Calhorda*[a]

Keywords: Molybdenum / Lamellar materials / Polymerization / Heptacoordination / Catalysis / ROMP

New lamellar materials intercalated with molybdenum(II) complexes with potential catalytic properties were prepared by a stepwise procedure. The lamellar material was first calcined at 823 K for four hours to eliminate all the carbonate ions; the layered structure was reconstructed after treatment with a solution of either pycH (pyridine-2-carboxylic acid) or $pydcH_2$ (pyridine-2,6-dicarboxylic acid) in a KOH solution of dmf at 343 K. Impregnation with a solution of the organometallic precursor $[Mo(CO)_3I_2(NCCH_3)_2]$ led to substitution of the nitrile groups by two pyridine ligands. All the materials were characterized by powder X-ray diffraction, FTIR, and ^{13}C CP MAS and ^{27}Al MAS solid-state NMR spectroscopy. Similar Mo^{II} complexes were also prepared by using pycH or $pydcH_2$ and characterized by elemental analysis as well as FTIR and ^1H and ^{13}C solution NMR spectroscopy. These new materials and the complexes of pyc or pydc ligands containing 4.54 wt.-% and 6.33 wt.-% of Mo respectively, catalyze the ring-opening-metathesis polymerization of norbornene and the polymerization of styrene at 333 K, their performance increasing upon the addition of methylalumoxane (MAO) as cocatalyst.

1. Introduction

Heterogeneous catalysis allows an easy separation of the products of a given reaction from the catalyst, being therefore favored in many industrial processes. The combination of organometallic complexes and a selected support has received much attention in recent years owing to the new perspectives it opens, since the first are known for their capabilities in selective and efficient promotion of many reactions in solution, while the latter optimize recovery and recycling of the catalysts.[1,2]

The choice of the supporting material and the incorporation of the organometallic precursor must be handled with care. In particular, porous materials are very promising candidates for such purposes, as they offer a large surface area inside the pores, but they must be designed by taking into consideration the need to afford a stable (and reactive) material without blocking the pores, so that the reaction can proceed and a good contact between the reactants is promoted.

Layered materials such as clays have been successfully used as hosts for the intercalation of other species. Layered double hydroxides (LDH), available as minerals or from synthesis and known as anionic clays, are very versatile. They can be thought of as descending from a $M(OH)_2$ hydroxide, such as $Mg(OH)_2$, with a structure built from layers of $Mg(OH)_6$ edge-sharing octahedra; if some of these Mg^{2+} dications are replaced by M^{3+} cations, the layers become positively charged, and anions are needed to balance this charge. They occupy, along with water molecules, the space between layers, and can be exchanged with other anions, organic or inorganic. Hydrotalcite (HTC) is an anionic clay from this family, based on Mg and Al cations, but a wide range of compositions $[M^{2+}_{1-x}M^{3+}_x(OH)_2](A^{m-})_{x/m}\cdot nH_2O$ (M^{2+} = Mg^{2+}, Zn^{2+}, Ni^{2+}, etc., M^{3+} = Al^{3+}, Cr^{3+}, Ga^{3+}, etc.) is possible.[3,4]

A rich intercalation chemistry can be obtained not only from the anion exchange process, but also from the substitution of the di- and trivalent cations in the layers. When sizes are not too different, the initial type of structure (brucite) does not change. The value of x, measuring the amount of M^{3+} relative to (M^{3+} + M^{2+}), is related to the distance between layers. This distance changes when other anions are introduced, although the layered structure is able to swell in the case of large anions, making space available between layers. Among the possible strategies for exchanging anions, rehydration of a calcined precursor has proved advantageous compared to direct anion exchange,[3] as competition between anions can be more efficiently pre-

[a] Departamento de Química e Bioquímica, CQB, Faculdade de Ciências da Universidade de Lisboa,
1749-016 Lisboa, Portugal
Fax: +351-217500088
E-mail: mjc@fc.ul.pt
cmnunes@fc.ul.pt
[b] Departamento de Engenharia Cerâmica e do Vidro, CICECO, Universidade de Aveiro,
Campus de Santiago, 3810-193 Aveiro, Portugal
Supporting information for this article is available on the WWW under http://www.eurjic.org or from the author.

vented as long as carbonate, the anion found in the minerals, is excluded. Several groups have worked along these lines, intercalating organic and inorganic anions, from simple to complicated biological ones.[3–5] In another interesting route, the synthesis of the double hydroxide is carried out in the presence of the anions chosen to belong to the final structure.[6,7]

These anions, despite their origin, can undergo several reactions, namely coordination to a metal center, provided that suitable functional groups are present. The calcined HTC itself has also been shown to catalyze reactions such as the aziration of oxiranes.[8] In this work, we studied the intercalation of pyridine-2-carboxylate and pyridine-2,6-dicarboxylate in a Mg/Al HTC and the reaction of the supported anions with a Mo^{II} precursor $[Mo(CO)_3I_2(NCCH_3)_2]$ (**1**), in order to evaluate the catalytic activity of the final materials in the heterogeneous polymerization of olefins. This was compared with the catalytic activity of the homogeneous analogue in the same reaction and the activity of related Mo^{II} complexes supported in other matrices.[9]

2. Results and Discussion

2.1. Characterization of the Complexes

The precursor complex $[Mo(CO)_3I_2(NCCH_3)_2]$ (**1**)[10] was allowed to react with two equivalents of either pycH or $pydcH_2$ (Scheme 1), affording the complexes formulated as $[Mo(CO)_3I_2(pycH)_2]$ (**2**) and $[Mo(CO)_3I_2(pydcH_2)_2]$ (**3**), respectively, as outlined in Scheme 2.[11,12]

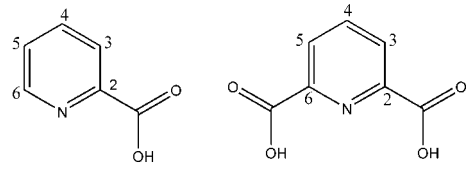

Scheme 1.

The ^1H NMR spectrum of $[Mo(CO)_3I_2(pycH)_2]$ (**2**) shows clear differences from those of the precursor complex **1** and the pycH ligand, namely the absence of a resonance at ca. 2.0 ppm assigned to the acetonitrile ligands of **1**, reflecting the loss of both acetonitrile ligands.

The four signals of the 6-H, 4-H, 3-H, and 5-H atoms (see numbering in Scheme 1) of the coordinated pycH ligand are observed at 8.99, 8.71, 8.66, and 8.37 ppm, respectively, clearly shifted relative to the corresponding signals in the free ligand at 8.76, 8.03, 8.10, and 7.67 ppm. The downfield shift experienced by the signals of the complexed ligand can be explained by the coordination to the electron-rich Mo center. The ^{13}C NMR spectrum confirms the above observations. Indeed, in the coordinated pycH, the resonances at 149.5, 144.2, 142.4, 131.3 and 129.0 ppm are assigned to the C-6, C-4, C-2, C-5, and C-3 atoms of the pyridine ring, while the carboxylate carbon atom appears at δ = 161.2 ppm. These values are shifted relative to those for the free ligand by small [149.4 ppm (C-6), 124.6 ppm (C-3)] and large amounts [137.4 (C-4), 148.4 (C-2), 126.7 (C-5), 166.1 ppm (carboxylate carbon)]. All these values are collected in Table 1.

The FTIR spectrum of $[Mo(CO)_3I_2(pycH)_2]$ (**2**) also reveals the absence of the $\nu_{C\equiv N}$ stretching modes at ca. 2300 cm^{-1} (Table 2). Another strong evidence for the substitution of the nitrile ligands is the strong redshift (lower wavenumbers) experienced by the $\nu_{C\equiv O}$ modes relative to the bands in complex **1**. The appearance of four bands at 2018, 1959, 1900, and 1845 cm^{-1}, assigned to the $\nu_{C\equiv O}$ modes, when only three were expected, was ascribed to the existence of another isomer in the solid. This situation has also been reported previously for the parent compound (Figure 1).[13] In order to evaluate the possible fluxionality between both isomers, complex **2** was dissolved in methanol, and the vibrational spectrum of this solution was recorded. The four bands are still visible in solution, as shown in Figure S1 in the Supporting Information, and are reflected in the difference spectrum compared with that of $[Mo(CO)_3I_2(pycH)_2]$ (**2**).

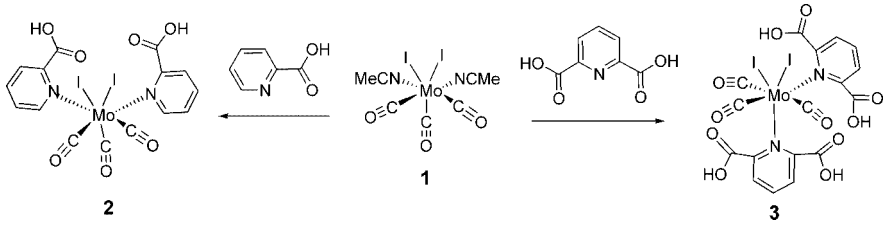

Scheme 2.

Table 1. ^1H and ^{13}C NMR chemical shifts [ppm] for the ligands pycH and $pydcH_2$, and the complexes **2** and **3**.

	3-H	4-H	5-H	6-H	C-2	C-3	C-4	C-5	C-6	COOH
pycH	8.10	8.03	7.67	8.76	148.4	124.6	137.4	126.7	149.4	166.1
2	8.66	8.71	8.37	8.99	142.4	129.0	144.2	131.3	149.5	161.2
$pydcH_2$	8.28	8.23	8.28	–	148.0	127.4	139.2	127.4	148.0	165.4
3	8.39	8.27	8.39	–	150.2	130.0	141.2	130.0	150.2	167.1

Table 2. FTIR wavenumbers of the $\nu_{C\equiv O}$, $\nu_{C=O}$, and $\nu_{C=N}$ modes for the ligands pycH and $pydcH_2$, and the complexes **1**, **2**, and **3**.

Complex or ligand	$\nu_{C\equiv O}$ [cm^{-1}]	$\nu_{C=O}$ [cm^{-1}]	$\nu_{C=N}$ [cm^{-1}]
$[Mo(CO)_3I_2(NCCH_3)_2]$ (**1**)	2017 (vs), 1924 (broad, vs)	–	–
pycH	–	1722 (vs)	1609 (vs), 1596 (vs)
$pydcH_2$	–	1701 (vs)	1468 (s), 1416 (s)
$[Mo(CO)_3I_2(pycH)_2]$ (**2**)	2018 (m), 1959 (s), 1900 (s), 1845 (s)	1740 (s)	1654 (s), 1612 (m)
$[Mo(CO)_3I_2(pydcH_2)_2]$ (**3**)	2071 (s), 2011 (s), 1943 (s)	1696 (vs)	1458 (m), 1413 (m)

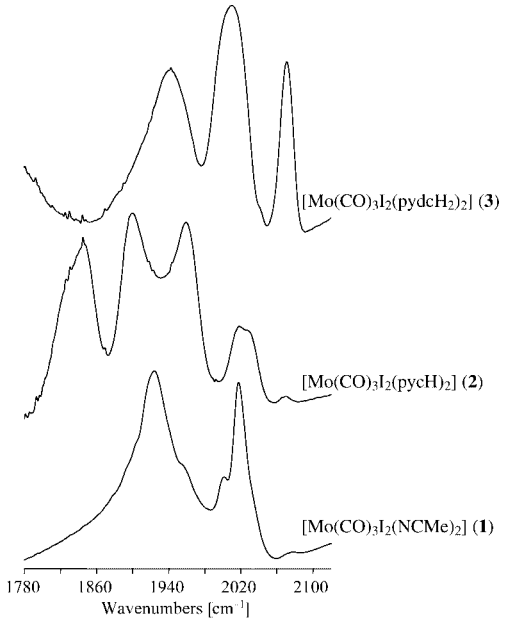

Figure 1. FTIR spectra of $[Mo(CO)_3I_2(NCCH_3)_2]$ (**1**), $[Mo(CO)_3I_2(pycH)_2]$ (**2**), and $[Mo(CO)_3I_2(pydcH_2)_2]$ (**3**).

The vibrational spectrum of complex **3** also supports its formulation as $[Mo(CO)_3I_2(pydcH_2)_2]$. The FTIR spectrum of $[Mo(CO)_3I_2(pydcH_2)_2]$ (**3**) shows only three narrow bands assignable to a single isomer, a fact that can be explained by the larger bulk of the two nitrogen ligands. They are slightly shifted relative to those of the precursor complex **1**. The $\nu_{C=O}$ mode of the $pydcH_2$ ligand shifts from 1701 cm^{-1} (in the free ligand) to 1696 cm^{-1} in complex **3**, while two bands assigned to the $\nu_{C=N}$ mode at 1468 (ν_{sym}) and 1416 cm^{-1} (ν_{asym}) in the free ligand undergo a redshift to 1458 and 1413 cm^{-1}, respectively, after binding.

In what concerns the ligand, the major changes should involve the $\nu_{C=N}$ of the ring and $\nu_{C=O}$ of the COOH group. The band at 1740 cm^{-1} ($\nu_{C=O}$ modes of the COOH group) in **2** shows a small blueshift of ca. 18 cm^{-1}, suggesting no involvement in hydrogen bonding. The $\nu_{C=N}$ modes of the free pycH ligand (1596 and 1609 cm^{-1}) shift upon complexation to 1612 and 1654 cm^{-1}, respectively.

The most relevant spectroscopic features of complex **2** are summarized in Table 2, as well as the corresponding data for complex **3**, the precursor complex **1**, and the ligands pycH and $pydcH_2$.

The ^1H NMR spectrum of complex $[Mo(CO)_3I_2(pydcH_2)_2]$ (**3**) is similar to the one described for **2**, with resonances at δ = 8.39 (3-H, 5-H) and 8.27 ppm (4-H), shifted to higher δ values relative to those observed for the free ligand (δ = 8.28 ppm for 3-H and 5-H; 8.23 ppm for 4-H). The pyridine signals in the ^{13}C NMR spectrum appear at 150.2, 141.2, and 130.0 ppm, being assigned to C-2/C-6, C-4, and C-3/C-5, respectively, while the COOH carbon is observed at δ = 167.1 ppm. All the signals are shifted downfield in comparison with free $pydcH_2$ [148.0 (C-2/C-6); 139.2 (C-4), and 127.4 ppm (C-3/C-5); COOH 165.4 ppm].

2.2. Intercalation of the Ligands and the Organometallic Fragment in Hydrotalcite

Prior to the intercalation experiments, the commercial HTC (**4**) lamellar material was submitted to a calcination process at 823 K for 4 h to eliminate the CO_3^{2-} anions in the interlayer region, as described previously.[8] The structure of the lamellar material collapses, but it is rebuilt in the following step, when the deprotonated ligands pyc and pydc are intercalated inside the intergallery space by using dmf at 343 K.[6] This procedure made possible the preparation of composite materials HTC–pyc (**5**) and HTC–pydc (**6**), containing the anions in the interlayer space, according to Scheme 3.

The results of elemental analyses of materials **5** and **6** show that the C/N mol ratios are 5.6 and 6.6, respectively, which are slightly higher than the expected values, 5.2 in pyc and 6.0 in pydc. On the other hand, the C/H mol ratios are 3.4 and 2.6, much lower than the expected values of 7.2 and 6.0. This suggests that incorporation of some carbonate during reconstruction of the layered structure leading to a multiphase sample does not take place.[14] Instead, the high content of hydrogen may be explained by the uptake of OH groups. On the basis of the amount of nitrogen for the two materials **5** and **6**, the contents of pyc and pydc ligands incorporated are 57% and 63%, respectively.

These functionalized materials were then allowed to react with the organometallic precursor **1** in dry CH_2Cl_2 for 24 h at room temperature, affording the new materials HTC–pyc–Mo (**7**) and HTC–pydc–Mo (**8**) after filtration and drying. The molybdenum loadings for the organometallic composite materials **7** and **8** were found to be 4.54 wt.-% and 6.3 wt.-% (0.43 mmol g^{-1} and 0.66 mmol g^{-1}), respectively, showing that higher metal quantities were incorporated in comparison to immobilization in a mesoporous support.[9] These results indicate the coordination of the available supported ligands to molybdenum to form 2:1 complexes, such as **2** and **3**.

All the new materials were characterized by powder XRD, FTIR, and solid-state ^{13}C and ^{27}Al NMR spectroscopic techniques.

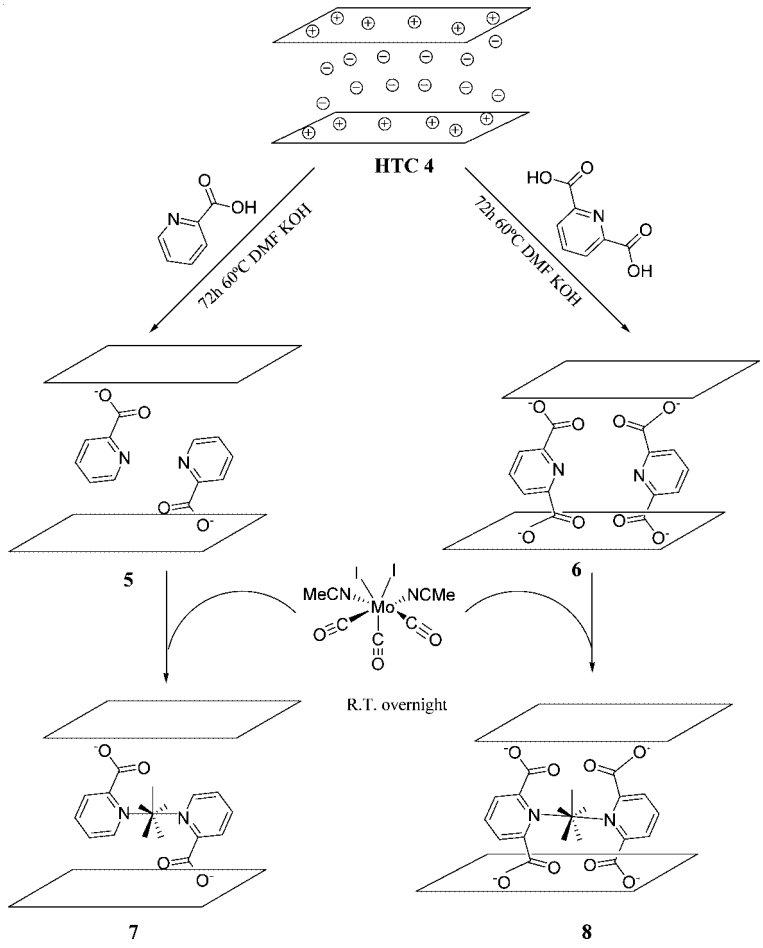

Scheme 3.

The powder XRD patterns obtained for these lamellar materials are typical of this type of reasonably well-ordered materials, exhibiting sharp and symmetric 003 reflections (Figure 2).[15]

The peaks were indexed to a rhombohedral symmetry. There was evidence of $Al(OH)_3$ in the lamellar materials, arising from the presence of gibbsite, at 2θ = 17.5, 28.9, and 39.2°. The calculated *d* parameters were 15.3 Å for the lamellar material **5** and 12.2 Å for material **6**. The 15.3 Å value found for material **5** corresponds to a gallery height of 10.5 Å, assuming the HTC sheets to be 4.8 Å thick.[3] Considering the longest dimension of the pycH guest to be approximately 8.8 Å, the value estimated for benzoate,[3] the XRD results suggest that a bilayer-like structure is assembled within the gallery. Furthermore, since the gallery height is only slightly superior to the size of the guest, the bilayer arrangement might consist of superimposed guest molecules, as schematized in Figure 3. Similar proposals have already been discussed by some authors.[3,15]

In the case of material **6**, the gallery height was found to be 7.4 Å. Assuming the length of the $pydcH_2$ guest (similar to a terephthalate anion) to be 9.9 Å, it is most likely that the molecules cannot be upright. They may either lie in a

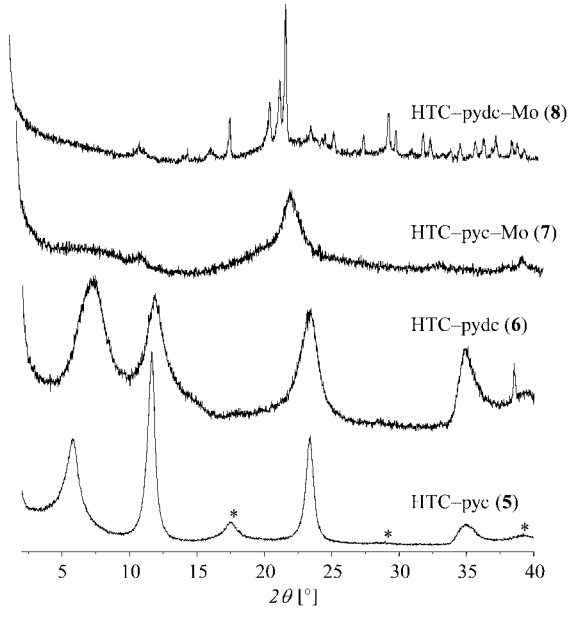

Figure 2. Powder XRD patterns of HTC–pyc (**5**), HTC–pydc (**6**), HTC–pyc–Mo (**7**), and HTC–pydc–Mo (**8**); * denotes peaks from gibbsite.

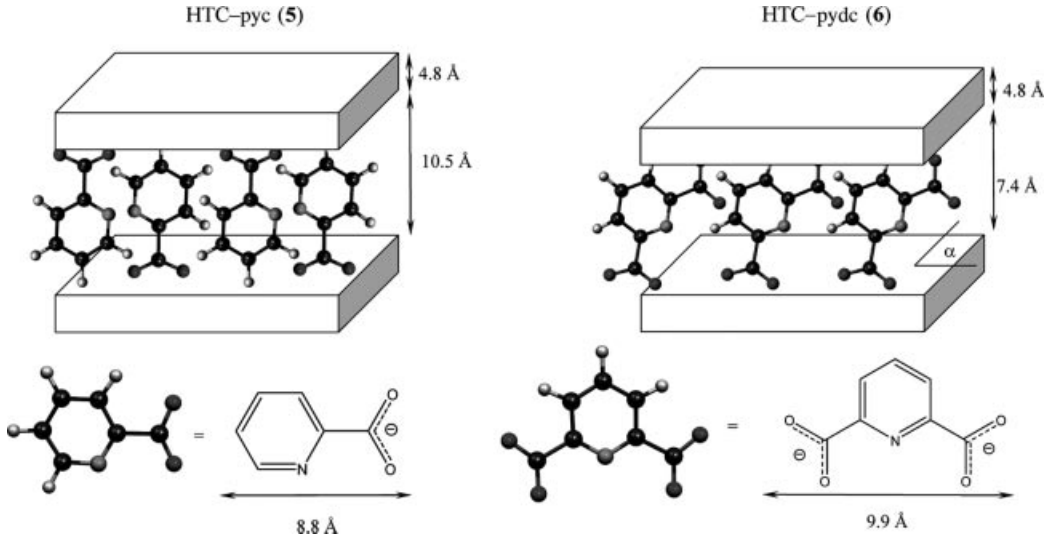

Figure 3. Models for the interlayer arrangement of the guest species of the materials HTC–pyc (**5**) and HTC–pydc (**6**); a color version of this figure is part of the Supporting Information.

horizontal arrangement, such as described in previous works,[3,15] or prefer tilted positions, up to a maximum tilt angle of 48° (α in Figure 3). This is also supported by the large full width at half height of the diffraction peaks.[15] The XRD patterns of materials **5** and **6** are very similar in terms of the number and positions of peaks, and differ mainly in the band width: broader peaks are observed for material **6**.

For materials **7** and **8**, obtained after treatment with complex **1**, the 001 reflections are significantly reduced in intensity. These changes can be attributed to a marked increase in the electron density at the midpoint of the interlayers due to the presence of the Mo centers at a high loading (4–6 wt.-%). This is in line with previous reports.[16,17] It is also possible, according to other reports, that the structure has partially disrupted owing to exfoliation, especially in material **8**.[18]

The FTIR spectrum of the HTC host material is similar to that of other materials of the same type. In the high-frequency region (4000–2000 cm^{-1}), it is dominated by broad bands at about 3400 cm^{-1}, assigned to the O–H stretches of weakly hydrogen-bonded water molecules and layer hydroxy groups. Some carbonate groups, from the air and humidity, may be responsible for the band at around 1400 cm^{-1}.The derivatized materials HTC–pyc (**5**) and HTC–pydc (**6**), resulting from the treatment of HTC with pyc and pydc anions, respectively, showed new bands in their vibrational spectra relative to the host material HTC. For HTC–pyc (**5**), a band at 3458 cm^{-1} is assigned to the O–H stretches of the structure of HTC and water molecules, as described above, the bands at 1598 and 1594 cm^{-1}, to the $\nu_{C=N}$ of the pyridine ring, and the band at 1632 cm^{-1} to the $\nu_{C=O}$ group of the carboxylate group of the ligand. Some of these bands show a deviation relative to the free ligand, because the ligand is deprotonated and held inside the gallery of the material. For HTC–pydc (**6**), it is possible to assign the bands at 2982 and 2977 cm^{-1} to the ν_{C-H} of the ring and the $\nu_{C=N}$ mode of the pyridine ring at 1439 and 1376 cm^{-1} (at 1468 and 1416 cm^{-1} in the free ligand). The band at 1607 cm^{-1} can be assigned to the $\nu_{C=O}$ mode of the ligand (1701 cm^{-1} in the free ligand). The small changes observed in the bands of both composite materials suggest that the structures of the anionic ligands were not affected during immobilization in the material.

Treatment of the composite materials **5** and **6** with the organometallic complex $[Mo(CO)_3I_2(NCCH_3)_2]$ led to the new materials HTC–pyc–Mo (**7**) and HTC–pydc–Mo (**8**). In the composite material **7**, the vibrations of the carbonyl groups ($\nu_{C\equiv O}$) at 2022, 1950, and 1880 cm^{-1} are shifted relative to those of complex **2**, probably as a result of specific host–guest interactions between the $Mo(CO)_3$ core and the layers of the HTC-derivatized host material. The $\nu_{C=N}$ modes of the pyridine ring appear at 1640 and 1630 cm^{-1}. These values are higher than those for the free ligand (1609 and 1596 cm^{-1}) and are close to those for complex **2**, indicating chelation to the metal center. The same trends are observed in HTC–pydc–Mo (**8**), with the $\nu_{C\equiv O}$ modes of the $Mo(CO)_3$ fragment at 2037, 1955, and 1892 cm^{-1}, and the $\nu_{C=N}$ modes of the pyridine ring at 1442 and 1395 cm^{-1}, values slightly lower than those for the free ligand (1468 and 1416 cm^{-1}), and close to the values for complex **3**. No bands that might be assigned to the $\nu_{C\equiv N}$ modes, observed at 2304 and 2277 cm^{-1} in the precursor **1**, corresponding to the acetonitrile ligands, were detected in either HTC–pyc–Mo (**7**) or HTC–pydc–Mo (**8**).

The ^{13}C CP MAS NMR spectra of the lamellar materials **5**–**8** (Figure 4) exhibit several resonances in the $120 < \delta < 150$ ppm range assigned to carbon atoms of the pyridine ring, and a single peak in the $160 < \delta < 170$ ppm range assigned to the carboxylate carbon atoms. These results indicate that the ligands are inside the interlamellar space of hydrotalcite for materials **5** and **6**. The sharp signals ob-

served for material **5** are similar to those found in solution for the pycH ligand, and can therefore be assigned: 124.7 (C-3), 128.0 (C-5), 139.8 (C-2), 146.6 (C-4), and 150.9 (C-6), and 170.1 ppm (*C*OO$^-$ group). In material **6**, the spectrum is not so well resolved. Three peaks at δ = 125.1, 139.2, and 150.2 ppm are attributed to the pyridine ring of the pydc ligand, and another at δ = 170.5 ppm for the *C*OO$^-$ group.

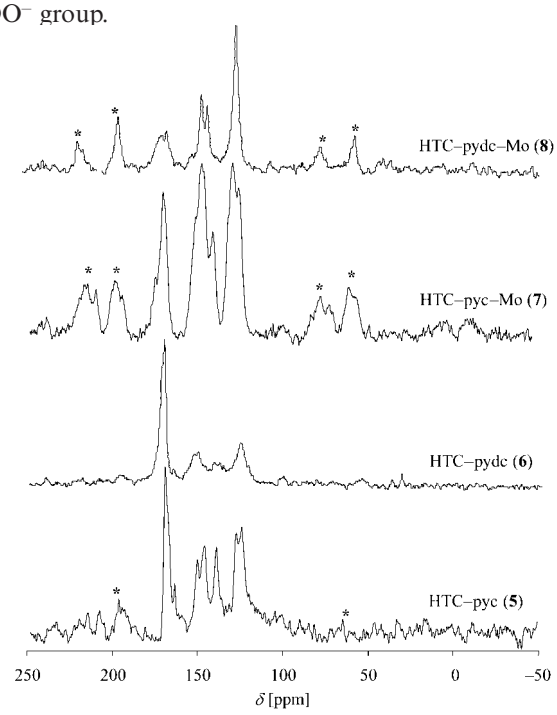

Figure 4. ^{13}C CP MAS NMR spectra for the materials HTC–pyc (**5**), HTC–pydc (**6**), HTC–pyc–Mo (**7**), and HTC–pydc–Mo (**8**); * denotes spinning side bands.

In materials **7** and **8**, no resonances of the acetonitrile ligands of precursor **1** are detected, and signals from the C≡O ligands are not visible, since they have a long relaxation time. On the other hand, the signals of the pyc ligand in **7** are not as clear as in the precursor **5**: 170.3 (*C*OO$^-$ group), 124.9 (C-3), 128.6 (C-5), 140.4 (C-2), and 147.0 ppm (C-4), whereas C-6 is convoluted with C-4. In material **8**, only three signals are resolved, namely the signals of the pyridine ring at δ = 127.1, 143.9, and 147.2 ppm, and that of the COO$^-$ group at δ = 167.4 ppm, as also observed for material **6**.

The ^{27}Al MAS NMR spectra of all the lamellar materials are very similar. A sharp peak is observed at ca. 9 ppm, with a broad downfield shoulder, assigned to octahedral aluminum. Similar spectra are described in the literature.[19] The first site, corresponding to the sharp peak, displays a distribution of isotropic chemical shifts and is probably due to the presence of a range of slightly different local Al environments generated by the random insertion of Al in the layers. The low-frequency shoulder corresponds essentially to undistributed Al species, but it has an average quadrupole coupling constant that is larger than that of the first site. This has been ascribed previously to small clusters of Al atoms in the brucite-like layers.[7]

2.3. Polymerization Catalytic Studies

Following the interest in the study of olefin polymerization catalyzed by Mo^{II} and W^{II} systems over the last years,[11–15] complex **1** has been tested for ring-opening-metathesis polymerization (ROMP) catalysis of norbornene and norbornadiene (NBE and NBD, respectively; polyNBE and polyNBD denote the corresponding polymer product).[11] ROMP of NBD has been successfully carried out by complexes $[Mo(CO)_3(NCCH_3)_2X_2]$ at room temperature for X = Br, while for X = I, a cocatalyst such as $ZrCl_4$ or $AlCl_3$ is required in order to initiate polymerization.[11] Recently, some of these Mo^{II} and W^{II} complexes immobilized in a MCM–41 material have also shown weak activity towards the ROMP reactions of NBE and NBD.[9] MAO has been successfully used as a cocatalyst in heterogeneous clay/metal systems as described in previous publications addressing olefin polymerization.[20,21]

In the present work, complexes **2** and **3** as well as materials **7** and **8** were tested for ROMP catalysis of NBE and polymerization of styrene (STY) at 333 K, and the results are collected in Table 3. The effect of addition of a cocatalyst (MAO) on the catalytic performance and the nature of the polymer were also checked. Complexes **2** and **3** show comparable activities towards both olefins, stressing that there is no beneficial effects of using either pycH or $pydcH_2$ ligands. This same trend is observed when MAO is used.

In absence of the cocatalyst, the composite materials **7** and **8** are slightly more active catalysts for the polymerization reaction of STY than the homogeneous counterparts **2** and **3**, while the results are comparable in the case of ROMP of NBE. The presence of aluminum in the sheets of the host material may contribute to a higher Lewis acidity and therefore induce a more efficient catalysis. This situation has already been discussed previously.[9,22–24]

Neither the calcined HTC host material nor the derivatized materials **5** and **6** possess catalytic activity towards the polymerization reactions of the olefins, indicating that the active species must contain molybdenum.

For all metal-containing catalysts and in the absence of the cocatalyst, the polymerization of STY is easier to accomplish than ROMP of NBE. Nevertheless, when MAO is used, the performances are boosted, more significantly for NBE than for STY, and polymer yields of polyNBE are higher than those found for polySTY. In fact, addition of MAO increases the yield of polySTY by an average factor of 3, while for polyNBE this factor reaches an average of 27.5. This general increase in yield is expected because of the role of MAO as a radical initiator, promoting the formation of the initial active species that binds to the metal center where the propagation and/or termination steps occur.

Another interesting factor is the local structure of the polymer, as homotactic isomers are preferred, namely in the case of polySTY, because of their industrial importance.[22,23] For polyNBE, a reasonable *cis* content is achieved in all the catalytic processes, but the *cis* content rises significantly in the presence of MAO. Thus, addition

Table 3. Results for the polymerization reactions of NBE and STY initiated by isolated and immobilized $[Mo(CO)_3I_2(L)_2]$ complexes at 333 K.

Catalyst	Cocatalyst	PolyNBE		PolySTY	
		Yield [%]	*cis* [%]	Yield [%]	*syndio* [%]
$[Mo(CO)_3I_2(pycH)_2]$ (**2**)	–	3	50	9	20
	MAO	99	50	31	20
$[Mo(CO)_3I_2(pydcH_2)_2]$ (**3**)	–	3	45	8	62
	MAO	91	60	24	65
HTC–pyc–Mo (**7**)	–	4	33	23	22
	MAO	95	44	60	65
HTC–pydc–Mo (**8**)	–	4	38	25	47
	MAO	94	56	61	42
MCM–DAB–Mo[a]	–	36	–	–	–
	MAO	59	–	–	–

[a] DAB = $(OEt)_3Si(CH_2)_3N{=}C(Ph){-}C(Ph){=}N(CH_2)_3Si(OEt)_3$, Mo = $MoBr_2(CO)_3$; from ref.[9]

of MAO is helpful not only in terms of reaction initiation, but also in directing the formation of homotactic polymer structures.

In the case of polySTY, the trend in the percentage of the syndiotactic polymer structure is not as clear, and MAO does not seem to influence the percentage of homotactic structures very much. As a general rule, and despite some good values of syndiotactic polymer yield (see Table 3, entries 3, 4, and 6), there is a general tendency towards the preparation of *syndio*-rich atactic polymers.

All the species described above exhibit higher catalytic activities towards the ROMP of NBE than the related Mo^{II} and W^{II} complexes immobilized in a MCM–41 material (Table 3, last entry).

3. Conclusions

The intercalation of heptacoordinate halocarbonylmolybdenum(II) complexes in organic–inorganic hybrid clay materials was successfully accomplished by first intercalating carboxylic acid derivatives of pyridine, under basic conditions, into the interlayer spacing of previously calcined hydrotalcite clay and subsequently introducing an organometallic fragment. This scheme was confirmed by several analytical techniques. For instance, FTIR spectra exhibited the bands assigned to $\nu_{C\equiv O}$ modes, reflecting the incorporation of the organometallic *fac*-$Mo(CO)_3$ core, and others showing the coordination of Mo to the pyridine ligand. Powder X-ray diffraction patterns, on the other hand, revealed the reconstruction of the HTC layered structure.

The catalytic activity in the ROMP reaction of NBE and polymerization of STY improves upon going from the homogeneous-phase complexes **2** and **3** to the corresponding heterogenized catalysts (**7** and **8**). In general, the conversions are higher for STY than for NBE. When MAO is added as a cocatalyst, the polymer yields are increased for both, so that the only obvious advantage of the heterogeneous catalysts seems to be the ease of separation.

A high content of *cis* polymer is detected for polyNBE, and the *cis* content increases when the reaction is carried out in the presence of MAO. There is no such simple trend for polySTY. The local structures of the polySTY may be better defined as *syndio*-rich atactic polymer chains.

Experimental Section

General: All preparations and manipulations were performed by using standard Schlenk techniques under nitrogen. Commercial grade solvents were dried and deoxygenated by standard procedures (Et_2O over Na/benzophenone ketyl; CH_2Cl_2, dmf, and CH_3CN over CaH_2), distilled under nitrogen, and kept over 4 Å molecular sieves (3 Å for CH_3CN). Picolinic acid (pycH), pyridine-2,6-dicarboxylic acid ($pydcH_2$), methyl alumoxane (MAO), and Mg,Al-hydrotalcite (HTC) were purchased from Aldrich Co. Prior to the intercalation experiments, commercial hydrotalcite was calcined (823 K for 4 h) in order to eliminate all the carbonate anions.[8] The precursor organometallic complex $[Mo(CO)_3I_2(NCCH_3)_2]$ (**1**) was also prepared according to literature methods.[10]

Powder XRD data were collected with a Phillips PW1710 diffractometer by using graphite-filtered Cu-K_α radiation. FTIR spectra were measured with a Nicolet Nexus 6700 FTIR spectrometer by using KBr pellets (for complexes) in the transmission mode and also with diffuse reflectance (for clay materials). Solution spectra were measured in a liquid cell with KBr windows and by using dry methanol as solvent. All FTIR spectra were measured with 2 cm^{-1} resolution.

^1H and ^{13}C solution NMR spectra were obtained at 400.13 MHz and 100.62 MHz, respectively, with a Bruker Avance 400 spectrometer by using CD_3OD as solvent. Chemical shifts are quoted in ppm from TMS.

^{27}Al and ^{13}C solid-state NMR spectra were recorded at 104.26 MHz and 100.62 MHz, respectively, with a (9.4 T) Bruker Avance 400P spectrometer. ^{13}C solid-state NMR spectra were also recorded at 125.76 MHz with a Bruker Avance 500P spectrometer. ^{27}Al MAS NMR spectra were acquired by using short and powerful radio-frequency pulses (0.6 μs, corresponding to π/12 pulses), a spinning rate of 14 kHz, and a recycle delay of 1 s. Chemical shifts are quoted in ppm relative to $[Al(H_2O)_6]^{3+}$. ^{13}C CP MAS NMR spectra were recorded with a 4.5-μs ^1H 90° pulse, 2-ms contact time, a spinning rate of 8 kHz, and 4-s recycle delays. Chemical shifts are quoted in ppm from TMS. Microanalyses were performed at the University of Vigo and the University of Aveiro.

Catalytic Studies: The complexes and materials reported herein were tested in the ROMP of norbornene (NBE) and polymerization of styrene (STY) under a N_2 atmosphere at 333 K and by using toluene as solvent. The catalytic reactions with complexes **2** and **3** were carried out by using a catalyst/olefin mol ratio of 1:200. In the studies with the composite materials **7** and **8**, a Mo/olefin mol ratio of 1:200 (based on the metal loadings as determined by ICP–

AES) was used. For the catalytic reaction with MAO as cocatalyst, the Mo/Al/olefin mol ratio was 1:3:200. In a typical experiment, a certain amount of the materials containing olefin (18.5 mmol) was mixed in toluene (10 mL) at 333 K. All the reactions were stopped after 48 h. This was accomplished by separating the catalysts by filtration, followed by the addition of methanol to the toluene solution in order to precipitate the polymer. The polymers were precipitated by addition of methanol at the end of the reaction, i.e., after 48 h and upon catalyst separation. The solid polymer was separated by filtration, and the polymers were dried in vacuo before being weighed. The yields were calculated on the basis of the initial weight of olefin used. The identification of the polymers was accomplished by ^{1}H NMR spectroscopy, and the *cis* content (NBE) and tacticity (STY) were estimated from ^{1}H and ^{13}C NMR spectroscopic data.[24,25–29]

Preparation of the Complexes $[Mo(CO)_3I_2L_2]$ (L = pycH or pydcH$_2$) (2, 3): A solution of $[Mo(CO)_3I_2(NCCH_3)_2]$ (**1**) (0.50 mmol, 258 mg) in CH_2Cl_2 (10 mL) was treated with a solution of the ligand pycH or pydcH$_2$ (1 mmol; 123 or 167 mg) in CH_2Cl_2 (5 mL). The resulting solution was stirred for 14 h at room temperature. The desired complex precipitated, and the solvent was filtered off. The complex was then washed with hexane and dried under vacuum.

$[Mo(CO)_3I_2(pycH)_2]$ (2): Yield: 92%. $C_{15}H_{10}I_2MoN_2O_7$ (680.00): calcd. C 26.49, H 1.48, N 4.12; found C 26.05, H 1.62, N 4.27. IR (KBr): $\tilde{\nu}$ = 3094 (m), 3052 (w), 2069 (vw), 2018 (m), 1959 (m), 1900 (m), 1845 (m), 1740 (s), 1654 (s), 1612 (vs), 1576 (m), 1559 (m), 1460 (s), 1340 (m), 1294 (s), 1206 (m), 1166 (m), 1092 (m), 962 (m), 757 (vs), 708 (m), 690 (m), 656 (w), 448 (w) cm^{-1}. ^{1}H NMR (400.13 MHz, $CDCl_3$, room temp.): δ = 8.99 (d, $J_{5,6}$ = 5.6 Hz, 1 H, pyc), 8.71 (t, $J_{4,5}$ = 8.0 Hz, 1 H, pyc), 8.66 (d, $J_{3,4}$ = 7.6 Hz, 1 H, pyc), 8.37 (t, $J_{5,6}$ = 6.6 Hz, 1 H, pyc) ppm. ^{13}C NMR (100.62 MHz, $CDCl_3$, room temp.): δ = 161.2 (COOH), 149.5 (C-6), 144.2 (C-4), 142.4 (C-2), 131.7 (C-5), 129.0 (C-3) ppm.

$[Mo(CO)_3I_2(pydcH_2)_2]$ (3): Yield: 96%. $C_{17}H_{10}I_2MoN_2O_{11}$ (768.02): calcd. C 26.59, H 1.31, N 3.65; found C 26.09, H 1.26, N 3.44. IR (KBr): $\tilde{\nu}$ = 3447(w), 3068 (w), 2901 (w), 2624 (w), 2546 (w), 2071 (w), 2011 (m), 1943 (m), 1696 (vs), 1654 (s), 1575 (m), 1458 (m), 1413 (m), 1331 (m), 1298 (m), 1266 (m), 1176 (w), 1080 (m), 997 (m), 915 (m), 855 (m), 752 (s), 702 (s), 648(s) cm^{-1}. ^{1}H NMR (400.13 MHz, $CDCl_3$, room temp.): δ = 8.27 (d, $J_{3,4}$ = 7.2 Hz, 1 H, pydc), 8.39 (d, $J_{4,5}$ = 7.6 Hz, 2 H, pydc) ppm. ^{13}C NMR (100.62 MHz, $CDCl_3$, room temp.): δ = 167.1 (COOH), 150.2 (C-2, C-6), 141.2 (C-4), 130.0 (C-3, C-5) ppm.

Preparation of the Materials HTC–L (L = pyc or pydc) (5, 6): A mixture of pycH (7.30 mmol) or pydcH$_2$ (3.60 mmol) in freshly distilled dmf (10 mL) and deionized water (20 mL) with NaOH (1 equiv. for pycH or 2 equiv. for pydcH$_2$) was stirred until complete solubilization. This solution was then added to a suspension of calcined HTC (1.00 g) in freshly distilled dmf (25 mL) at 343 K, and the reaction mixture was stirred at the same temperature for 48 h. All the manipulations were carried out under a N_2 atmosphere to prevent the uptake of carbonate anions. The resulting material was then filtered off, washed with deionized water (3 × 20 mL), and dried in a desiccator under vacuum.

HTC–pyc (5): Elemental analysis found: C 13.65, H 4.05, N 2.41. IR (KBr) $\tilde{\nu}$ = : 3458 (vs), 1632 (s), 1598 (s), 1476 (m), 1374 (s), 1293 (w) cm^{-1}. ^{13}C NMR CP MAS NMR: δ = 124.7 (C-3), 128.0 (C-5), 139.8 (C-2), 146.6 (C-4), 150.9 (C-6), 170.1 (COOH) ppm. ^{27}Al MAS NMR: δ = 9.47 ppm.

HTC–pydc (6): Elemental analysis found: C 10.19, H 3.98, N 1.55. IR (KBr): $\tilde{\nu}$ = 2982 (vs), 2977 (vs), 2907 (s), 1607 (s), 1563 (s), 1439 (m), 1376 (vs), 1269 (w), 1174 (w), 1083 (w), 957 (m), 771 (s), 676 (s), 566 (m), 450 (s) cm^{-1}. ^{13}C NMR CP MAS NMR: δ = 125.1 (C-3, C-5), 139.2 (C-4), 150.2 (C-2, C-6), 170.5 (COOH) ppm. ^{27}Al MAS NMR: δ = 9.28 ppm.

Preparation of the Materials HTC–L–Mo (L = pyc or pydc) (7, 8): A solution of $[Mo(CO)_3I_2(NCCH_3)_2]$ (**1**) (0.34 g, 0.65 mmol) in dry CH_2Cl_2 (5 mL) was added to a suspension of the HTC intercalated material HTC–L (**4** or **5**) (1.00 g) in dry CH_2Cl_2 (20 mL). The reaction mixture was stirred under a N_2 atmosphere at room temperature for 24 h. The resulting material was then filtered off, washed with CH_2Cl_2 (2 × 20 mL), and dried in a desiccator under vacuum.

HTC–pyc–Mo (7): Elemental analysis found: C 7.36, H 2.66, Mo 4.54, N 1.32. IR (KBr) $\tilde{\nu}$ = 3460 (vs), 2972 (w), 2947 (w), 2875 (w), 1950 (m), 1640 (s), 1630 (s), 1480 (m), 1380 (m), 1300 (w), 962 (m), 679 (s), 447 (s) cm^{-1}. ^{13}C CP MAS NMR: δ = 124.7 (C-3), 128.0 (C-5), 139.8 (C-2), 146.6 (C-4), 150.9 (C-6), 170.1 (COOH) ppm. ^{27}Al MAS NMR: δ = 9.97 ppm.

HTC–pydc–Mo (8): Elemental analysis found: C 5.19, H 3.14, Mo 6.33, N 0.96. IR (KBr): $\tilde{\nu}$ = 3480 (m), 2180 (m), 2180 (w), 2037 (vw), 1955 (vw), 1892 (vw), 1680 (vs), 1617 (vs), 1442 (m), 1395 (s), 1294 (m), 1198 (w), 1084 (m) cm^{-1}. ^{13}C CP MAS NMR: δ = 127.1 (C-3, C-5), 143.9 (C-4), 147.2 (C-2, C-6), 164.66 (COOH) ppm. ^{27}Al MAS NMR: δ = 9.67 ppm.

Supporting Information (see footnote on the first page of this article): FTIR spectra of $[Mo(CO)_3I_2(NCCH_3)_2]$ (**1**), $[Mo(CO)_3I_2(pycH)_2]$ (**2**), complex **2** in MeOH solution and the difference spectrum of complex **2** and MeOH; color version of Figure 3.

Acknowledgments

C. D. N. and P. D. V. thank Fundação para a Ciência e a Tecnologia (FCT) for research grants (SFRH/BPD/14512/2003) and (SFRH/BPD/14903/2004), respectively. The authors are grateful to FCT and FEDER for grant POCTI/QUI/44654/2002.

[1] M. H. Valkenberg, W. F. Hölderich, *Catal. Rev.* **2002**, *44*, 321–374.
[2] A. Taguchi, F. Schüth, *Microporous Mesoporous Mater.* **2005**, *77*, 1–45.
[3] a) S. P. Newman, W. Jones, *New J. Chem.* **1998**, *22*, 105–115 and the references cited therein; b) S. P. Newman, S. J. Williams, P. V. Coveney, W. Jones, *J. Phys. Chem. B* **1998**, *102*, 6710–6719 and the references cited therein.
[4] A. I. Khan, D. O'Hare, *J. Mater. Chem.* **2002**, *12*, 3191–3198.
[5] J.-C. Dupin, H. Martinez, C. Guimon, E. Dumitriu, I. Fechete, *Applied Clay Sci.* **2004**, *27*, 95–106.
[6] S. Gago, M. Pillinger, A. A. Valente, T. M. Santos, J. Rocha, I. S. Gonçalves, *Inorg. Chem.* **2004**, *43*, 5422–5431.
[7] S. Gago, M. Pillinger, T. M. Santos, J. Rocha, I. S. Gonçalves, *Eur. J. Inorg. Chem.* **2004**, 1389–1395.
[8] G. Negrón, N. Guerrra, L. Lomas, R. Gaviño, J. Cárdenas, *ARKIVOC* **2003**, *xi*, 179–184.
[9] J. Gimenez, C. D. Nunes, P. D. Vaz, A. A. Valente, P. Ferreira, M. J. Calhorda, *J. Mol. Catal. A: Chem.* **2006**, *256*, 90–98.
[10] P. K. Baker, S. G. Fraser, E. M. Keys, *J. Organomet. Chem.* **1986**, *309*, 319–321.
[11] C. D. Nunes, M. Pillinger, A. A. Valente, J. Rocha, A. D. Lopes, I. S. Gonçalves, *Eur. J. Inorg. Chem.* **2003**, 3870–3877 and references cited therein.
[12] C. D. Nunes, M. Pillinger, A. A. Valente, A. D. Lopes, I. S. Gonçalves, *Inorg. Chem. Commun.* **2003**, *6*, 1228–1233.
[13] P. K. Baker, M. B. Hursthouse, A. I. Karaulov, A. J. Lavery, K. M. A. Malik, D. J. Muldoon, A. Shawcross, *J. Chem. Soc., Dalton Trans.* **1994**, 3493–3498.

[14] S. Carlino, *Solid State Ionics* **1997**, 73–84.
[15] J.-C. Dupin, H. Martinez, C. Guimon, E. Dumitriu, I. Fechete, *Applied Clay Sci.* **2004**, *27*, 95–106.
[16] P. Beaudot, M. E. De Roy, J. P. Basse, *Chem. Mater.* **2004**, *16*, 935–945.
[17] S. Gago, M. Pillinger, R. A. Sá Ferreira, L. D. Carlos, T. M. Santos, I. S. Gonçalves, *Chem. Mater.* **2005**, *17*, 5803–5809.
[18] R. Ma, Z. Liu, L. Li, N. Iyi, T. Sasaki, *J. Mater. Chem.* **2006**, *16*, 3809–3813.
[19] J. Rocha, M. del Marco, V. Rives, M. A. Ulibarri, *J. Mater. Chem.* **1999**, *9*, 2499–2503.
[20] S. Ray, G. Galgali, A. Lele, S. Sivaram, *J. Polym. Sci., Part A: Polym. Chem.* **2004**, *43*, 304–318.
[21] S. Bruzaud, Y. Grohens, S. Ilinca, J.-F. Carpentier, *Macromol. Mater. Eng.* **2005**, *290*, 1106–1114.
[22] D. Jamanek, A. Woyna, W. Skupiński, *Appl. Organomet. Chem.* **2002**, *16*, 575–579.
[23] F. Bao, R. Ma, X. Lü, G. Gui, Q. Wu, *Appl. Organomet. Chem.* **2006**, *20*, 32–38.
[24] H. Rahiala, I. Beurroies, T. Eklund, K. Hakala, R. Gougeon, P. Trens, J. B. Rosenholm, *J. Catal.* **1999**, *188*, 14–23.
[25] M. Al-Jahdali, P. K. Baker, A. J. Lavery, M. Meehan, D. J. Muldoon, *J. Mol. Catal. A* **2000**, *159*, 51–62.
[26] P. K. Baker, M. A. Beckett, B. M. Stiefvater-Thomas, *J. Mol. Catal. A* **2003**, *193*, 77–81.
[27] T. Szymanska-Buzar, T. Glowiak, I. Czelusniak, *J. Organomet. Chem.* **2001**, *640*, 72–78.
[28] T. Szymanska-Buzar, T. Glowiak, I. Czelusniak, *Polyhedron* **2002**, *21*, 2505–2513.
[29] I. Czelusniak, T. Szymanska-Buzar, *Appl. Catal., A* **2004**, *277*, 173–182.

Received: January 24, 2007
Published Online: May 9, 2007

